AD-755 925

SYNTHESIS OF RARE EARTH COMPOUNDS AND STUDY OF THEIR MAGNETIC OPTICAL AND SEMICONDUCTING PROPERTIES

F. Hotzberg, et al

IBM Watson Research Center

Prepared for:

Army Missile Command
Advanced Research Projects Agency

January 1973

SYNTHESIS OF RARE EARTH COMPOUNDS AND STUDY OF THEIR MAGNETIC OPTICAL AND SEMICONDUCTING PROPERTIES

IBM Corporation
Thomas J. Watson Research Center
Yorktown Heights, New York 10598

SEMIANNUAL TECHNICAL REPORT

January 1973

Contract No. DAAH01-70-C-1313

sponsored by

Advanced Research Project Agency
ARPA Order No. 1588

ARPA Support Office - Army Missile Command
Directorate for Research, Development
Engineering and Missile Systems Laboratory
U.S. Army Missile Command
Redstone Arsenal, Alabama

NOTICE

"This research was sponsored by the Advanced Research Projects Agency of the Department of Defense under ARPA Order No. 1588 and was monitored by the U.S. Army Missile Command under Contract No. DAAH01-70-C-1313. Views and conclusions expressed herein are the primary responsibility of the author or the contractor and should not be interpreted as representing the official opinion or policy of USAMICOM, ARPA, DOD or any other agency of the Government.

Unclassified

Security Classification

DOCUMENT CONTROL DATA - R & D

(Security classification of title, body of abstract and indexing annotation must be entered when the overall report is classified)

1. ORIGINATING ACTIVITY *(Corporate author)*
International Business Machines Corporation
Thomas J. Watson Research Center, P.O. Box 218
Yorktown Heights, New York 10598

2a. REPORT SECURITY CLASSIFICATION
Unclassified

2b. GROUP

3. REPORT TITLE
RESEARCH IN THE SYNTHESIS OF RARE EARTH COMPOUNDS AND A STUDY OF THEIR MAGNETIC OPTICAL AND SEMICONDUCTING PROPERTIES

4. DESCRIPTIVE NOTES *(Type of report and inclusive dates)*
Semiannual Technical Report (30 June 1972 to 31 December 1972)

5. AUTHOR(S) *(First name, middle initial, last name)*
F. Holtzberg, L. J. Tao, T. Penney, M. W. Shafer and S. von Molnar

6. REPORT DATE	7a. TOTAL NO. OF PAGES	7b. NO. OF REFS
January 1973	53	53

8a. CONTRACT OR GRANT NO.	9a. ORIGINATOR'S REPORT NUMBER(S)
DAAH01-70-C-1313	IBM Project #2567
b. PROJECT NO.	
c.	9b. OTHER REPORT NO(S) *(Any other numbers that may be assigned this report)*
d.	

10. DISTRIBUTION STATEMENT
Distribution of this document is unlimited

11. SUPPLEMENTARY NOTES	12. SPONSORING MILITARY ACTIVITY
	Advanced Research Project Agency Arlington, Virginia 22209 ARPA Order No. 1588

13. ABSTRACT The report is divided into three sections: the first section describes transport measurements in disordered ferromagnetic semiconductors, the second deals with magnetic exchange interactions in a mixed valence system of a non magnetic La^{+++} ion and Van Vleck Sm^{++} ion having a non magnetic ground state, and the third section presents results on intercalation of divalent rare earth ions into layer type structures.

Transport measurements have been made on the magnetic semiconductors $Gd_{3-x}v_xS_4$. The vacancies, v, are randomly distributed throughout the lattice and lead to fluctuating repulsive potentials and band tailings. Furthermore, since our largest measured carrier concentrations are small compared to the maximum number of vacancies ($\sim 2.3 \times 10^{21}$ cm^{-3}), a rigid band model should be applicable. This is in contrast to ordinary semiconductors where the energy dependence of the density of states is generally a strong function of the dopant concentration. Recent transport measurements in Eu doped EuS, which demonstrate the applicability of a model for transport in a band tail of localized states are reviewed. The two systems are compared and discussed in terms of a model first suggested by Cutler and Mott for paramagnetic $Ce_{3-x}v_xS_4$ and modified here to include magnetic interactions.

Even though Van Vleck ions have non-magnetic ground states, exchange interactions between them can be observed by magnetic susceptibility measurements. The principles of these measurements are described as well as a technique for accounting for the paramagnetic impurity contribution to χ_M. Measurements are reported in SmS doped with La, which show that the Sm^{2+}-Sm^{2+} exchange interaction is greatly enhanced by the conduction electrons donated by the La.

The rare earth metals Eu and Yb and the alkaline earth Sr have been intercalated

DD FORM 1 NOV 65 1473

Ic

Unclassified

Security Classification

Unclassified
Security Classification

14. KEY WORDS	LINK A		LINK B		LINK C	
	ROLE	WT	ROLE	WT	ROLE	WT
Semiconducting ferromagnets						
Synthesis						
Nonstoichiometry						
Crystal growth						
Rare earths						
Disordered systems						
Gadolinium Sesquisulfide						
Layer compounds						
Intercalation						

Ib

Unclassified
Security Classification

in the group IV and VI dichalcogenides with layer type structures. The intercalations were carried out at low temperatures in liquid ammonia solutions and were shown to be free of the ferromagnetic impurities $Eu(NH_2)_2$ and $Eu(NH_3)_6$. Lattice parameter increases in the c direction of the hexagonal cell, independent of the concentration of the intercalated species, from 18.39Å for pure 3R MoS_2 to 27.84 for the Eu intercalated material were measured. We find the intercalated species to go between every layer and ammonia is intercalated along with the metals. The composition of MoS_2 fully intercalated with Eu is $MoS_2(Eu)_{.9-1.0}(NH_3)_{1-1.5}$.

MoS_2 orders ferromagnetically at 4-5°K when intercalated with Eu in concentrations greater than $MoS_2(Eu)_{.5-.6}$. The ferromagnetic compositions have paramagnetic Curie temperatures of 8-9°K and Curie constants consistent with the europium being all divalent, i.e., C_M=7.9. When Yb and Sr are intercalated in MoS_2 superconductivity occurs at 2.8 and 5.2°K respectively.

IC

SYNTHESIS OF RARE EARTH COMPOUNDS AND STUDY OF THEIR MAGNETIC OPTICAL AND SEMICONDUCTING PROPERTIES

IBM Corporation
Thomas J. Watson Research Center
Yorktown Heights, New York 10598

SEMIANNUAL TECHNICAL REPORT

January 1973

Contract No. DAAH01-70-C-1313

sponsored by

Advanced Research Project Agency
ARPA Order No. 1588

ARPA Support Office - Army Missile Command
Directorate for Research, Development
Engineering and Missile Systems Laboratory
U.S. Army Missile Command
Redstone Arsenal, Alabama

Id

FOREWORD

This report describes work performed under contract DAAH01-70-C-1313 for the ARPA Support Office, Research, Development, Engineering and Missiles Laboratory, U. S. Army Missile Command, Redstone Arsenal, Alabama during the period 30 June 1972 through 31 December 1972. The monitor for this project was R. Norman. The principal investigator was F. Holtzberg and the report was written by F. Holtzberg, M. W. Shafer, L.J. Tao and S. von Molnar. Part of this work (the $Sm_{1-x}La_xS$ in colloboration with J. B. Torrance) was performed under joint auspice of ARPA and the ONR (N00014-70-C-0272). The work was performed at the IBM Thomas J. Watson Research Center. The authors gratefully acknowledge the technical assistance of R. A. Figat, R. B. Hamilton, H. R. Lilienthal, and P. G. Lockwood, and the support of R. W. Johnson, J. D. Kuptsis and W. Reuter who provided the following analytical techniques: Solid state mass spectroscopy and quantitative electron probe microanalysis.

SUMMARY

The report is divided into three sections: the first section describes transport measurements in disordered ferromagnetic semiconductors, the second deals with magnetic exchange interactions in a mixed valence system of a non magnetic La^{+++} ion and Van Vleck Sm^{+2} ion having a non magnetic ground state, and the third section presents results on intercalation of divalent rare earth ions into layer type structures.

Transport measurements have been made on the magnetic semiconductors $Gd_{3-x}v_xS_4$. The vacancies, v, are randomly distributed throughout the lattice and lead to fluctuating repulsive potentials and band tailings. Furthermore, since our largest measured carrier concentrations are small compared to the maximum number of vacancies ($\sim 2.3 \times 10^{21} cm^{-3}$), a rigid band model should be applicable. This is in contrast to ordinary semiconductors where the energy dependence of the density of states is generally a strong function of the dopant concentration. Recent transport measurements in Eu doped EuS, which demonstrate the applicability of a model for transport in a band tail of localized states are reviewed. The two systems are compared and discussed in terms of a model first suggested by Cutler and Mott for paramagnetic $Ce_{3-x}v_xS_4$ and modified here to include magnetic interactions.

Even though Van Vleck ions have non-magnetic ground states, exchange interactions between them can be observed by magnetic susceptibility measurements. The principles of these measurements are described as well as a technique for accounting for the paramagnetic impurity contribution to

χ_M. Measurements are reported in SmS doped with La, which show that the Sm^{2+}-Sm^{2+} exchange interaction is greatly enhanced by the conduction electrons donated by the La.

The rare earth metals Eu and Yb and the alkaline earth Sr have been intercalated in the group IV and VI dichalcogenides with layer type structures. The intercalations were carried out at low temperatures in liquid ammonia solutions and were shown to be free of the ferromagnetic impurities $Eu(NH_2)_2$ and $Eu(NH_3)_6$. Lattice parameter increases in the c direction of the hexagonal cell, independent of the concentration of the intercalated species, from 18.39Å for pure 3R MoS_2 to 27.84 for the Eu intercalated material were measured. We find the intercalated species to go between every layer and ammonia is intercalated along with the metals. The composition of MoS_2 fully intercalated with Eu is $MoS_2(Eu)_{.9-1.0}(NH_3)_{1-1.5}$.

MoS_2 orders ferromagnetically at 4-5°K when intercalated with Eu in concentrations greater than $MoS_2(Eu)_{.5-.6}$. The ferromagnetic compositions have paramagnetic Curie temperatures of 8-9°K and Curie constants consistent with the europium being all divalent, i.e., C_M=7.9. When Yb and Sr are intercalated in MoS_2 superconductivity occurs at 2.8 and 5.2°K respectively.

TABLE OF CONTENTS

LIST OF FIGURES

1.0 INTRODUCTION

The last annual technical report (DAAH01-71-C-1313, June 1972) presented the result of a study of the effects of disorder on transport properties of a series of non-stoichiometric EuS samples. The emphasis in this case was on the effects of localization on transport due to static potential fluctuations and it represented the first successful quantitative description of hopping transport in a band tail. It was possible in the EuS system, with the magnetic fields available, to separate magnetic and coulombic effects. In this report we describe transport measurements on the magnetic semiconductor $Gd_{3-x}v_xS_4$. Because of the large number of randomly distributed vacancies ($\sim 10^{21} cm^{-3}$) in these materials, they represent transitional phases between the well ordered crystalline and amorphous states. Unlike metastable amorphous systems, it is reasonable to assume, that it is possible to grow stable crystals of gadolinium sesquisulfide with variable vacancy concentrations under equilibrium conditions. In the second section we extend some of the ideas relating to electrons localized by coulombic disorder to include potential fluctuations of magnetic origin.

The next section deals with effects on magnetic exchange of conduction electrons donated by non magnetic La^{+++} ions to the Van Vleck ion Sm^{++} in SmS. In spite of the fact that Sm^{++} has a non magnetic ground state it has a sizeable susceptibility since its magnetic properties are determined by higher lying multiplet states. The principles of the susceptibility measurement are described as well as a technique for accounting for paramagnetic impurity contributions to χ_M.

The final section is concerned with a study of layer type transition metal dichalcogenides. These compounds are characterized by strongly

bonded sheets of ions which are loosely coupled by Van der Waals binding. It is this weak interlayer bonding which permits the intercalation of a variety of metallic species between the layers without disturbing the layer structure. We describe the low temperature intercalation of europium in MoS_2 and show that ytterbium and strontium can also be intercalated. The magnetic properties of the three intercalated systems are compared.

2.0 THE EFFECT OF COULOMBIC AND MAGNETIC DISORDER ON TRANSPORT IN MAGNETIC SEMICONDUCTORS

2.1 INTRODUCTION

Transport of charge carriers in many magnetic semiconductors is dominated by potential fluctuations of both coulombic and magnetic origin. In contrast to the coulombic case, the binding energies of states localized by spacial fluctuations in magnetic order may be both temperature and magnetic field dependent.[1,2,3]

This section reviews recent advances made in describing and understanding the physical properties of materials in which the electrons are localized by coulombic disorder and extends these ideas to magnetic materials. In particular we compare the properties of a magnetic semiconductor $Gd_{3-x}V_xS_4$ with its isostructural paramagnetic counterpart $Ce_{3-x}V_xS_4$. We hope to show that such a comparison is helpful in that it allows us to look at the anomalous properties of the magnetic solid in terms of the well established band tail model. We find that we can account qualitatively for our transport measurements by using this model.

For the case of materials where static potential fluctuations are invoked as the cause of disorder, e.g. amorphous or heavily doped non-magnetic semiconductors, the concentration for which defects and impurity wavefunctions overlap has been described in terms of band tailing.[4] The basic concept is that there exists a series of electronic states (See Fig. 1) below what was formerly the bottom of the unperturbed conduction band. Concomitant with this tail, there exists an energy, E_c, below which electrons are more or less immobile and have to move by hopping and above which the states are extended and the electron's movement is limited only by scattering. E_c is

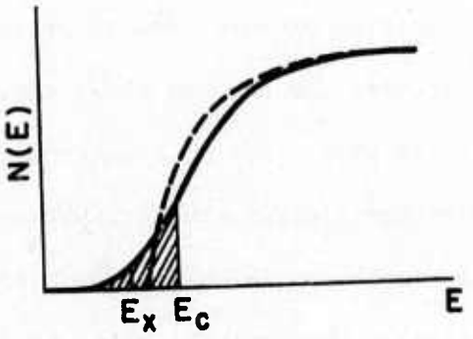

Figure 1 Density of State, N(E) vs energy for a disordered solid. The shaded area indicates localized states and the dashed line is the density of states for the ordered material. (After Cutler and Mott, Ref. 15).

a consequence of quite general considerations concerning electronic localization in a disordered lattice.[5] The electron localization depends critically on the magnitude of the potential fluctuation. For example, van Vechten[6] has recently concluded on theoretical grounds that no band tail is expected for covalent amorphous semiconductors, since the covalent bonds will tend to rearrange themselves in such a way as to minimize the distortion energy and thus preserve short range order. Band tailing was not detected experimentally in strain free amorphous Si and Ge.[7] On the other hand Busch, Campagna, and Siegmann[8] were able to show from an analysis of photothreshold in photoemission experiments that in ionic materials large band tails can be produced in the disordered state.

A severe limitation in most attempts to study transport of disordered semiconductors has been the lack of information about the energy dependence of the density of states and mobility. We would like to review here the salient features of transport analysis on three compounds in which the band tail has been well studied and its occupancy is relatively well controlled.

Redfield[9] has compared experimental data on heavily doped, closely compensated GaAs with a band tail model. His samples, all of which were doped to the same carrier concentration and later compensated, provided a "rigid" band tail, whose density of states, N(E), was not expected to change substantially between samples since the net carrier concentrations were smaller than the donor concentration by at least 2 orders of magnitude.[10] It was thus possible to calculate the conductivity, using the formula

$$\sigma(T) = \int N(E)\, f]E-E_F(T)]\mu(E)dE \qquad 2.1.1$$

where N(E) is the density of states, $f[E-E_F(T)] = f$ is the Fermi function and $\mu(E)$ is an energy dependent mobility. The prescription is, first, to assume a form for N(E) (which, in the case of GaAs, had been calculated to be Gaussian), to calculate $E_F(T)$, the temperature dependence of the Fermi energy, by using particle conservation, and then to try several functional forms for $\mu(E)$. Redfield[9] found remarkable agreement with his data[10] by choosing an energy dependent form for μ which was also a Gaussian tail.

Thompson, et al,[11] used a similar approach to analyze their data on the magnetic semiconductor EuS. It should be pointed out that these authors were focusing their attention on the non-magnetic transport properties of this compound and consequently quenched the magnetic field dependent resistivity peak near the ordering temperature by applying a field of 32 kOe. Their results for Eu-rich samples show that the data are well described by the following model: 1) conduction occurs in a "rigid" band tail (the tail is exponential rather than Gaussian); 2) <u>at high temperatures</u> $\mu(E)$ is energy and temperature dependent, $\mu(E) \alpha \exp[E_c-E)/kT]$; 3) the electrons deepest in the band tail do not contribute to the Hall effect; 4) at low temperature conduction is described by Mott's variable range hopping formula,[12] $\sigma=\sigma_o \exp(T_o/T)^{1/4}$, with T_o predicted from the high temperature data. An unexpected aspect of this work is that a rigid band tail model works as well as it does. The samples were chosen by varying the Eu/S ratio and one might expect N(E) to change substantially. Apparently there is some contribution of unknown defects common to all samples.

It is obvious from the above discussion that a form for N(E) must be found before one can make quantitative comparisons between theory and ex-

periment. Furthermore, consistency between samples can only be tested if a rigid band tail is assumed. On the other hand, a qualitative description of transport behavior is possible, even when N(E) is not known precisely, as long as we can be assured that the rigid band tail model is valid. A case in point is the system $Ce_{3-x}v_xS_4$, where the vacancies, v, are an intrinsic structural property of the solid. The interesting feature of this system is that one can fill the vacant sites with the same cation and thereby create charge carriers. In comparison with the large number of vacancies ($\sim 2.1 \times 10^{21}$), the carrier concentration can be varied over a significant range, presumably without seriously affecting the energy dependence of N(E). This system was studied experimentally by Cutler et al[13,14] and its transport properties were interpreted by Cutler and Mott.[15]

These compounds are only one of many rare earth Th_3P_4 type structures, and interest in them arises for at least two reasons: first of all, the $Ce_{3-x}v_xX_4$(X=S,Se,Te)($0 \leq x \leq 1/3$) compounds change continuously from metals to insulators with increasing vacancy concentration, x, leading to a variety of cooperative effects such as superconductivity and ferromagnetism;[16] secondly, the disordered distribution of vancancies at the Th sites (which are discussed below), is expected to lead to fluctuating repulsive potentials and tailing of the conduction band in which the electronic states are localized.[15]

In the following we describe some aspects of the Th_3P_4 structure and briefly review the arguments of Cutler and Mott[15] pertaining to their analysis of transport in the cerium compound. In Section II we present transport data obtained on samples of the isomorphic, but magnetic, compound $Gd_{3-x}v_xS_4$ and compare our measurements to the paramagnetic cerium

system. Section III presents our interpretation in terms of the concept of localization of electron states first suggested in Ref. 15, and extended here to include magnetic interactions.

The Th_3P_4 type structure was first described by Meisel.[17] In 1949 Zachariasen[18], on the basis of x-ray powder diffraction and density data, showed that the defect Ce_2S_3 compound crystallized with the Th_3P_4 structure, in the space group $I43d\text{-}T_d^6$ with four molecules per unit cell. In this space group the 12-fold cationic sites are fixed while the 16-fold anionic sites are determined by a parameter, μ. Both Zachariasen's and Meisel's analyses fixed the value of μ at 1/12 or 0.083. The deficit Ce_2S_3 was described by Zachariasen as having 10 2/3 Ce atoms statistically distributed over the twelve cation sites, whereas the sixteen fold anion sites were filled. On the basis of these results Zachariasen predicted that 4/3 vacant cation sites per unit cell could be filled and therefore the structure should exist over a single phase region extending from S:Ce=1.5 to S:Ce-1.33.

The coordination polyhedra were described in detail by Krpyakevich[19] and by Boltzberg and Methfessel.[20] Single crystal x-ray analysis on related materials[21,22] showed that the parameter μ for rare earth compounds was nearer to 0.075 which displaces the anion from its symmetrical position.

Recently Carter[23] suggested the possible existence of vacancy and charge ordering in Th_3P_4 defect type structures but concluded that there is insufficient experimental evidence to confirm the existence of vacancy ordering and it is not clear that the arguments for charge ordering are

conclusive. One might suspect, however, that it is unlikely to find adjacent cation vacancies and it is therefore reasonable to assume that some short range order exists. Although this would reduce the magnitude of the static potential fluctuations, the existence of a rigid band tail in Th_3P_4 structures is clearly a good assumption as long as the donor concentration is small compared to the total number of vacancies ($\sim 2.1 \times 10^{21}$ cm^{-3} in $Ce_{3-x}v_xS_4$).

The latter assumption is the basis for the analysis of transport data on $Ce_{3-x}v_xS_4$. Cutler and Mott[15] argue that when $E_F(0)$, the low temperature Fermi energy, lies below E_c, conduction is thermally activated and approaches 0, as $T \to 0$. When $E_F(0)$ is above E_c, conduction occurs in extended states and remains finite as T approaches 0. They also show, that, regardless of the mode of transport the fundamental equations for σ, the conductivity and S, the thermopower, can be written in the familiar form

$$\sigma = -\int \sigma(E)(\partial f/\partial E)dE \qquad 2.1.2$$

and

$$S\sigma = \frac{k}{e} \int \sigma(E) \frac{E-E_F}{kT} \partial f/\partial E \, dE \quad .^{15,4} \qquad 2.1.3$$

The function $-kT\partial f/\partial E = f(1-f)$ is centered about $E_F(T)$ of width kT, where k is Boltzmann's constant. Consequently the transport will depend very sensitively on the magnitude of $|E_c-E_F|$ compared to kT. Cutler and Mott then specialize their discussion to electron concentrations and temperature ranges where E_F lies in the region of localized states and where $E_c-E_F \gg kT$. They conclude that, when the electronic current is carried by states near E_F, the thermoelectric power, S, is given by

$$S = \frac{\pi^2}{3} \frac{k^2T}{e} \frac{d(\ell n\sigma)}{dE} \quad E=E_F. \qquad 2.1.4$$

This is the familiar metallic formula and when applied to thermally activated conduction of the form

$$\sigma = \sigma_o(E) \quad e^{-W(E)/kT} \quad , \qquad 2.1.5$$

where W(E) is the mean activation energy for hops, equation 2.1.4 yields

$$S = \frac{\pi^2}{3} \frac{k}{e} \left(kT \frac{d \ln \sigma_o}{dE} - \frac{dW}{dE} \right)_{D=E_F} . \qquad 2.1.6$$

When, however, the electronic current is negligible, i.e. $\sigma(E) \to 0$, for energies below some energy E_x, (See Fig. 1) the thermoelectric power takes on a form similar to that for semiconductors, i.e.

$$S = \frac{k}{e} \left(\frac{E-E_F}{kT} + \frac{1+2kT \; d \ln \sigma/dE + \ldots}{1+kT \; d \ln \sigma/dE + \ldots} \right)_{E=E_x} . \qquad 2.1.7$$

Equation 2.1.6 predicts linear behavior in T with non-zero intercept (contrary to the case for metals). This behavior is observed in moderately doped ($\sim 5 \times 10^{18}$-10^{19} cm^{-3}) $Ce_{3-x}V_xS_4$. The dependence on inverse temperature, Eq. 2.1.7, is observed in considerably more insulating samples containing 5-9×10^{17} carriers/cm^3. One particularly interesting sample ($n = 5.2 \times 10^{18}$ cm^{-3}) obeys Eq. 2.1.6 between $\sim$100 and 300°K, but changes to 1/T behavior at lower temperatures.[14] Presumably E_F changes wtih temperature in this ample and the quantity $E_c - E_F$ is small enough so that above $\sim$100°K much of the charge is transported either by hopping or in extended states (both would give a term for S linear in T). The reason we belabor this point is that similar behavior is observed in $Gd_{3-x}V_xS_4$ as shown in Fig. 4.

When $|E_c - E_F|$ and kT become comparable, as is apparently the case

in EuS[11], no approximate formula is valid and a full integration over energy has to be carried out to compare theory with experiment.[9,11] In $Gd_{3-x}V_xS_4$ we suppose that $|E_c-E_F|$ is not only a function of temperature and concentration but also a function of magnetization and we shall attempt to relate the experimental values for $\rho = 1/\sigma$ and S to this concept.

2.2 EXPERIMENTAL RESULTS FOR $Gd_{3-x}V_xS_4$

Single crystals of $Gd_{3-x}V_xS_4$ were grown by slowly cooling the melts (m.p. ~1800°C) contained in sealed tungsten crucibles to about 1000°C, annealing at that temperature for several hours and quenching to room temperature. Although we have not, thus far, determined the exact compositions of the materials it is clear that the Gd_2S_3 composition is insulating ($\rho > 10^6 \Omega$cm), transparent and anti-ferromagnetic and that the composition for which x≈0 the samples are metallic and ferromagnetic. Lattice parameters obtained with a Guinier focussing camera using Cu radiation are essentially constant throughout the single phase region with a_o=8.375±.002Å.

TABLE I

	Sample I.D.	n_∞(cm^{-3})	μ_{RT}(cm^2/v-sec)	ρ_{RT} (-cm)	θ(°K)
1.	24-118 (673)	†5.6 x10^{19}	1.25	9.45x10^{-2}	††-6.7 to -9.0
2.	24-60 (658)	*8.7±.8x10^{19}	2.5	2.5x10^{-2}	††8.6 to 11.7
3.	23-76 (594)	*1.6±.5x10^{20}	2.3	1.66x10^{-2}	16.1
4.	23-10	*2.5±.2x10^{20}	2.5	8.23x10^{-3}	22.2

† n_∞ is the value extrapolated to 1/T→0, on the assumption that μ=constant.

* $n_\infty \equiv \lim_{\chi \to 0} (10^{-8}/e)\div(e_H/H_A)$, where χ=susceptibility, e_H is the Hall resistivity, and H_A is the applied magnetic field.

†† These values were not determined on the specific samples used in transport but represent the variations for several crystals from the same crystal growth experiment.

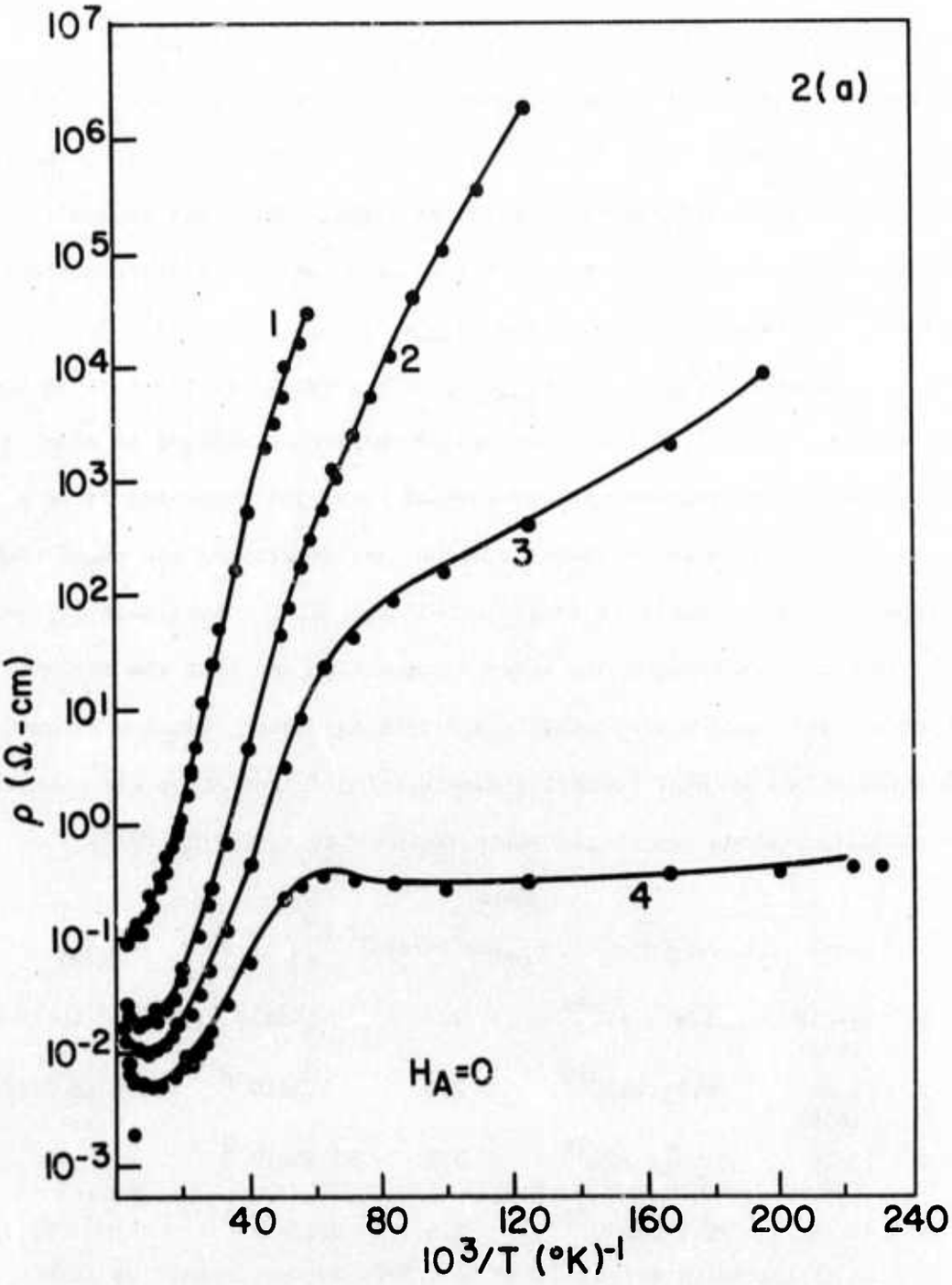

Figure 2 Electrical resistivity, ρ, of $Gd_{3-x}v_xS_4$ for varying compositions (See Table I) as a function of temperature, T; (a) with no external magnetic field applied, (b) in the presence of an applied field of 32 kOe.

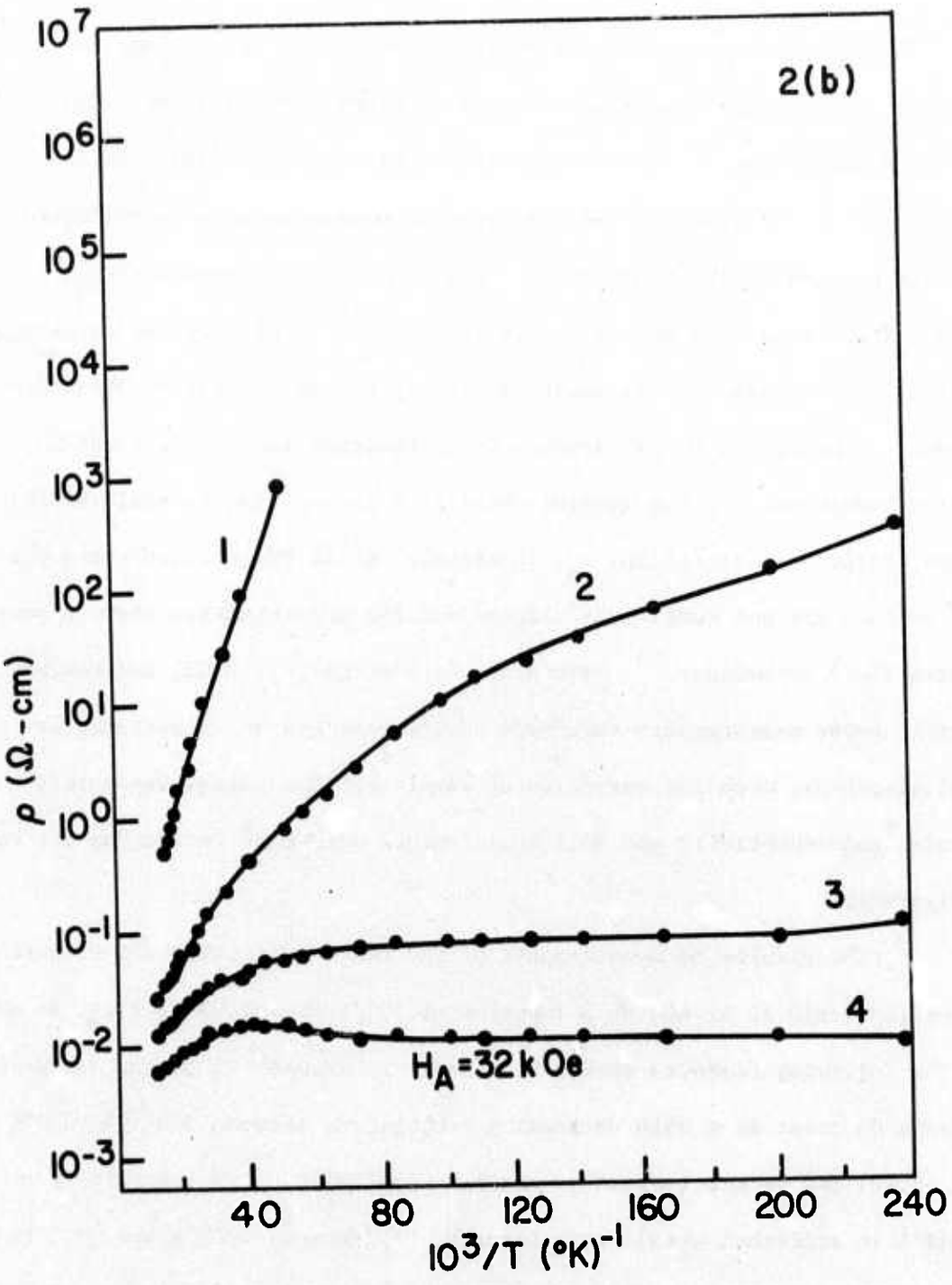

Figure 2 Electrical resistivity, ρ, of $Gd_{3-x}V_xS_4$ for varying compositions (See Table I) as a function of temperature, T; (a) with no external magnetic field applied, (b) in the presence of an applied field of 32 kOe.

Table I summarizes some physical properties of the samples studied. Preliminary measurements by us on samples 3 and 4 have been published previously.[24] The single crystal material does not show an easy direction for cleavage and the magnetic measurements were performed on small samples of arbitrary shape. For the present purposes the important features of the magnetic data are: a) the high temperature susceptibility, χ, follows a Curie Weiss law (resulting in the extrapolated Θ values, b) below $\sim$70°K, $1/\chi$ departs from linearity indicating possible cluster formation, c) the general trend is from negative to positive Θ's, as the carrier concentration, n_c, increases, d) in the ordered state the Gd^{3+} moments are not completely aligned and the magnetization shows a pronounced field dependence.[24] Five probe dc resistivity, Hall, and thermoelectric power measurements were made on crystals shaped as rectangular parallelopipeds, with the exception of sample 1. The latter was a thin platelet and resistivity and Hall measurements were made in the Van der Pauw configuration.

The results of measurements of the resistivity with and without an applied field of 32 kOe as a function of $10^3/T$ are shown in Figs. 2a and b. The following features should be noted: 1) Samples 2, 3, and 4 exhibit a linear decrease in ρ with decreasing temperature between 300 and $\sim$200°K (not shown) and have a resistance minimum near 100°K. The resistivity of sample 1 is activated at all temperatures. 2) Between $\sim$100°K and $\sim\Theta$, $\rho(H=0)$ is activated for samples 2, 3, and 4 but the activation energy changes significantly as Θ is approached. 3) Application of a magnetic field reduces ρ over the entire temperature range below $\sim$50°K in all samples. The curves

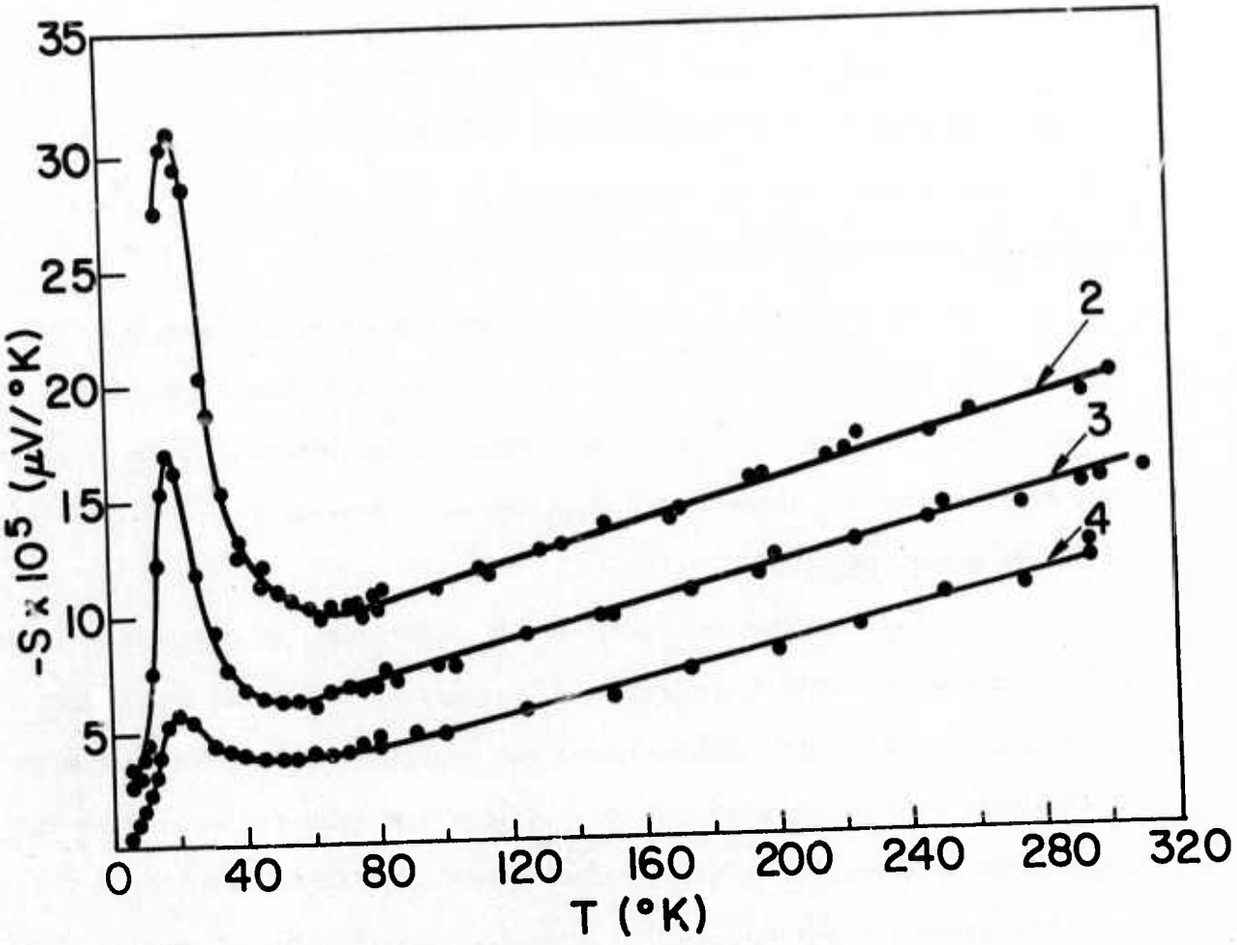

Figure 3 Thermoelectric power, S, of $Gd_{3-x}V_xS_4$, for varying compositions (See Table I) as a function of temperature T.

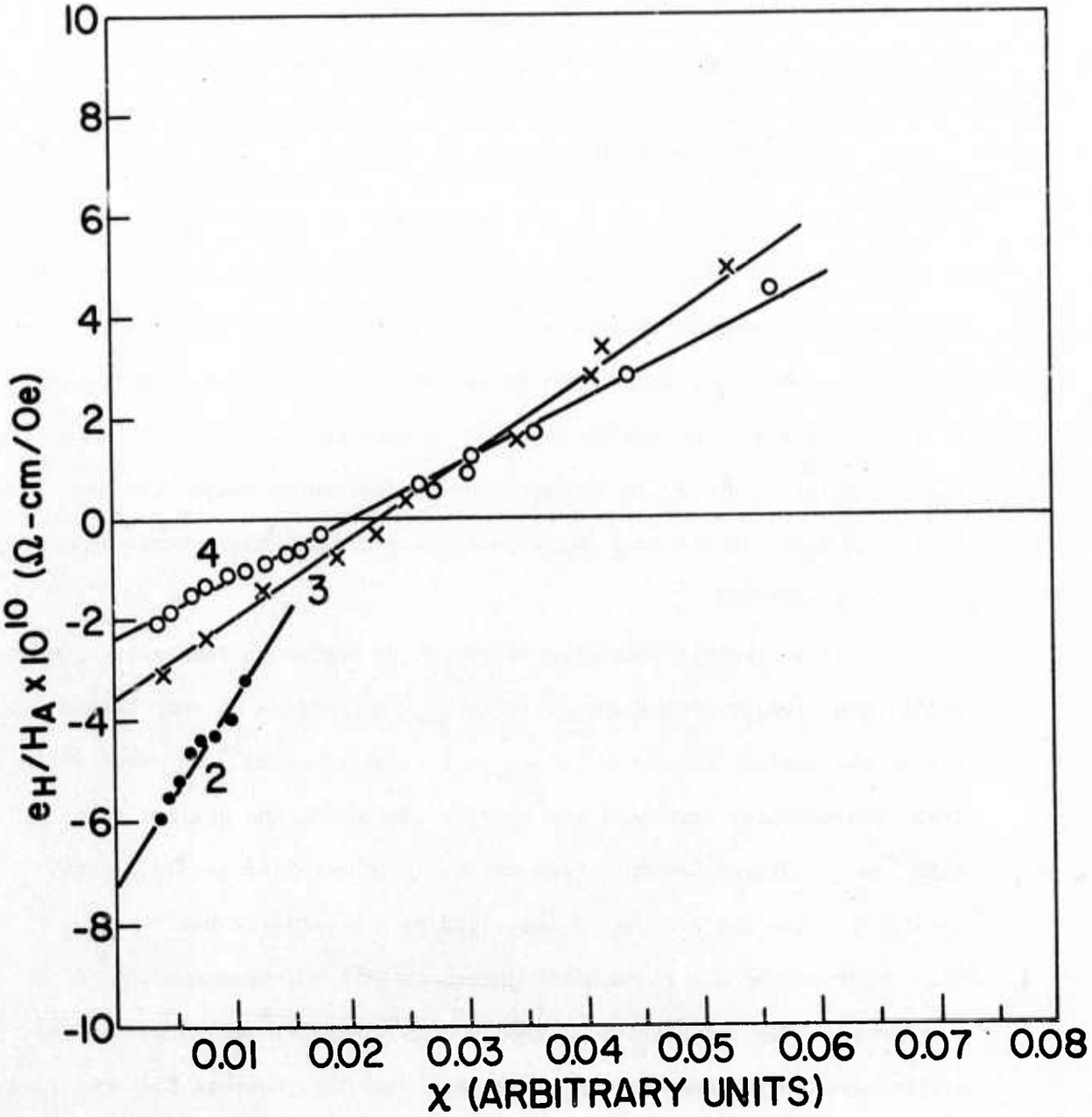

Figure 4 Hall coefficient, e_H/H_A, of $Gd_{3-x}V_xS_4$ for varying compositions (See Table I) as a function of magnetic susceptibility, χ.

$M=[\chi/(1+N\chi)]H_A = \chi^*H_A$, where N is the demagnetizing factor, to

$$\frac{e_H}{H_A} = R_o+[R_o(4\pi-N)+R_1]\chi^* \quad . \qquad 2.2.2$$

If it is assumed that R_o and R_1 are independent of temperature, then a plot of e_H/H_A vs $\chi^* \approx \chi$ should yield a straight line with R_o as intercept. This relationship is roughly obeyed for temperatures above 77°K as can be seen in Fig. 4. The values for n_∞ quoted in Table I are derived from the magnitude of R_o obtained in this manner. It is also obvious that, if our assumption regarding R_o and R_1 is correct, the conduction is n-type and the change in sign of e_H/H_A is due to a large positive anomalous Hall coefficient (R_1).

2.3 DISCUSSION

If we restrict our discussion to the region in temperature above ~100°K, the transport behavior of the $Gd_{3-x}v_xS_4$ samples is very similar to that of the cerium isomorph. In $Ce_{3-x}v_xS_4$, Cutler et al[14] observed activated, non-metallic transport for carrier concentrations smaller than $\sim 8\times10^{19}$ cm^{-3}. Higher concentration materials behave like metals for all temperatures and are adequately described by conventional band theory.[13] These observations are in complete agreement with our measurements on the Gd compound. The resistivity of sample 1 is thermally activated over the entire experimental temperature range (See Fig. 2a), whereas the resistivities of samples 2 through 4 initially decrease linearly with temperature as the samples are cooled from ~300°K (This effect is indicated by the apparent resistivity minimum towards the left of the figure). The fact that $n_\infty > 8\times10^{19}$ cm^{-3} for samples 2-4 is in excellent agreement with Cutler and Levy's observations in $Ce_{3-x}v_xS_4$[14], although this result is possibly fortuitous,

since the lattice parameter in the Ce compound is somewhat larger than in the Gd compound. It does, however, confirm our earlier remark that the low temperature behavior of samples 2-4 must be dominated by magnetic effects. The result also suggests that E_F lies near, but above E_C in our samples 2-4, whereas $E_F<E_C$ for sample 1. The latter then appears to be similar to the non-metallic EuS samples studied in detail by Thompson et al[11], and we shall concentrate further discussion on samples 2-4.

The thermoelectric power, S, is linear with an intercept which decreases with increasing carrier concentration, n. For sample 4, then, it seems reasonable to assume the unperturbed density of states indicated by the dashed line in Fig. 1 and to find E_F from the slope of S vs T. This result is readily derived from Eq. 2.1.4, if we assume $\sigma(E)=\text{const } E^x$. In this case

$$S = \frac{\pi^2}{3} \frac{k^2 Ty}{3 e E_F} \quad . \qquad 2.3.1$$

If y=1, consistent with the assumption that lattice and neutral impurity scattering dominates the resistance, $E_F \simeq .07$eV. The density of states effective mass m*, defined as

$$m^* = \frac{\hbar^2}{2 E_F} (3\pi^2 n)^{2/3} \quad , \qquad 2.3.2$$

is $\sim 1.6 m_e$, where m_e is the free electron mass. This value is smaller than similar calculations on $Ce_{3-x}V_xS_4$.[13] E_F cannot be determined for samples 2 and 3 from the linear part of S because $|E_F-E_c| \leq kT$ over much of the experimental range and current carriers from both above and below E_c contribute to S. Equation 2.1.2 thus should be evaluated numerically. This requires, as we pointed out earlier, a knowledge of the functional form for N(E). Although we lack this information for $Gd_{3-x}V_xS_4$, Thompson[28] has

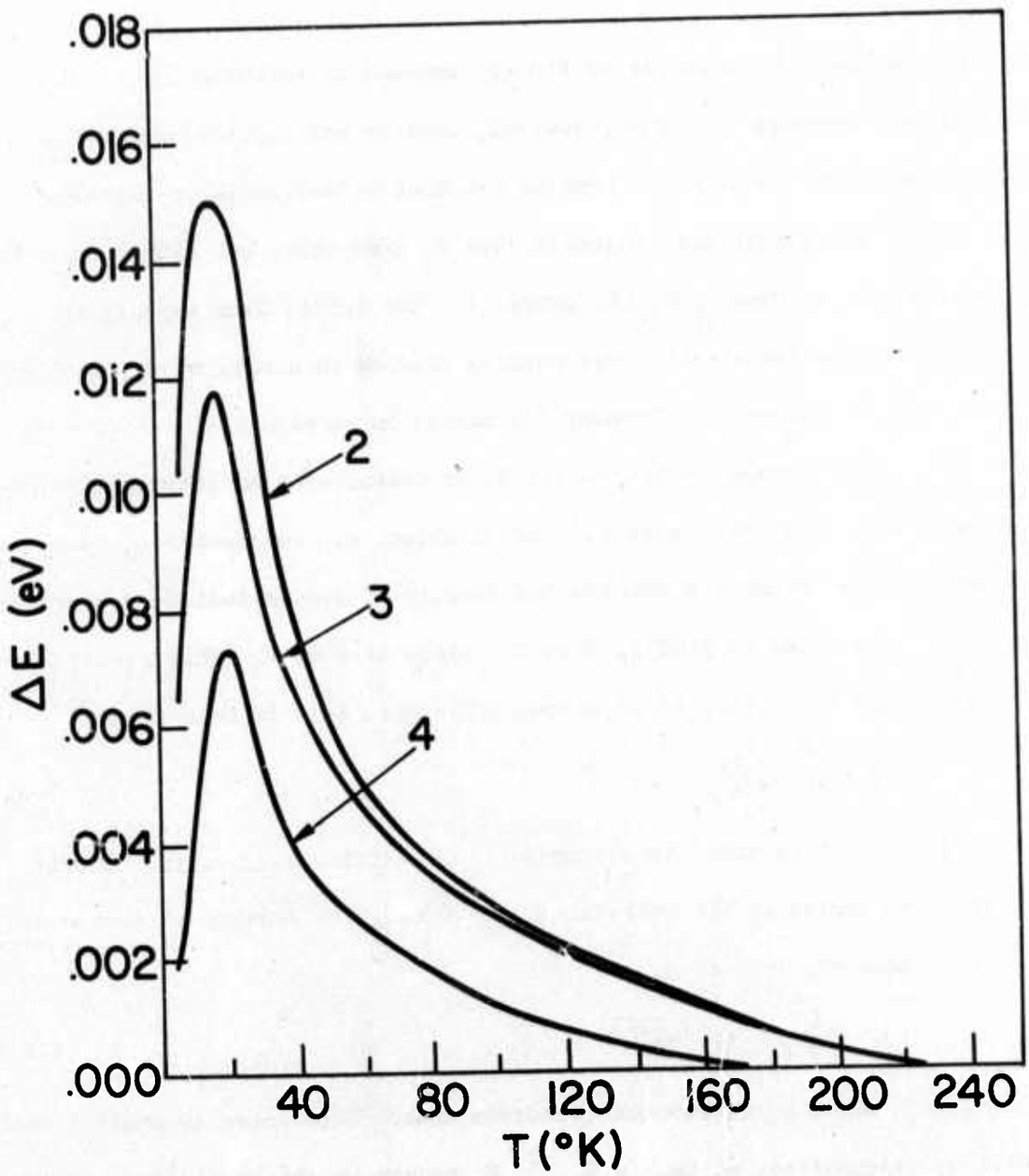

Figure 5 Activation energy for electrical resistivity, ΔE, of $Gd_{3-x}v_xS_4$ calculated from the data (Fig. 2a).

calculated S(T) for one of the EuS samples described in Ref. 11. His calculation is in good agreement with our experimental values for S on the same EuS sample.[29]

From the foregoing discussion we might expect small changes in Hall constant in samples 2 and 3, since the electron distribution above E_c is expected to change with temperature. If n, and consequently the normal Hall coefficient, R_o, is changing, the effect is completely masked in our experiments by R_1. Furthermore, measurements of R_o in EuS exhibit surprisingly weak temperature dependences for dopant concentrations and temperatures such that $|E_c-E_F| \lesssim kT$. Guided by this result and the data of Cutler and Levy[14] we have confidence that our extrapolation procedure for obtaining n_∞ is reasonable.

Whereas the Ce and Gd compounds behave very similarly at high temperature, $Gd_{3-x}v_xS_4$ exhibits new magnetization dependent phenomena at low temperatures. In order to study these magnetic effects at temperatures below ~200°K we have analyzed our resistivity data in terms of an activation energy, $\Delta E(T)$, in a manner similar to Penney, et al[30]. We assume, on the basis of the $Ce_{3-x}v_xS_4$ results and our high temperature data, that samples 2-4 would remain metallic in the absence of magnetic interactions and define $\Delta E(T)$ from the data $\sigma(T)$ by

$$\sigma(T) = \sigma_M(T)e^{-\Delta E/kT} \quad , \qquad 2.3.3$$

where $\sigma_M(T)$ is roughly of the form A+BT, with A and B specified by the linear high temperature behavior. $\Delta E(T)$ is then computed from $\sigma(T)$ point by point for all temperatures. Our results are shown in Fig. 5.[31]

The peaks in ΔE occur in the neighborhood of but slightly higher

than the measured Θ values. Although the curves are not shown, ΔE is substantially reduced by an applied magnetic field, i.e. when ΔE is derived from the data of Fig. 2b. It follows that ΔE is an activation energy for conduction which is related to magnetic order. We have implicitly neglected effects on the mobility due to critical scattering. This is justified, since the changes in resisitivity are too large to be accounted for by scattering theory and since, in our model, transport occurs predominantly by hopping near the Curie temperature Θ.

Our hypothesis for the change in ΔE, which we claim to be primarily magnetic in samples 2-4, has its origin in the idea of magnetic polaron bound by the Coulomb field of a donor or vacancy first discussed by Kasuya[2]. Torrance has developed this concept and applied it to the insulator-metal transition in EuO[3] and the resisitivity peak in EuS.[32] The cause for the localization is the exchange interaction, I_{c-f}, between the conduction electron and the localized Gd^{3+} 4f spins. The magnetic binding energy is related to I_{c-f} $(\langle S\rangle_{cluster} - \langle S\rangle_{lattice})$, where the term in brackets expresses the difference in average magnetization between a cluster of spins in the neighborhood of an electron and spins elsewhere in the magnetic lattice. This term encourages an electron in the coulomb field of a defect to contract forming a small magnetic spin cluster.[2,3] Furthermore, the combined effect of both magnetic and Coulomb interactions make the localized state stable over relatively wide temperature ranges.[33]

Regardless of the microscopic mechanism of localization, the bracketted term in the magnetic binding energy explains several features of ΔE observed experimentally in $Gd_{3-x}V_xS_4$. If we assume, for simplicity,

that $\langle S \rangle_{cluster} \approx S$, i.e. the ferromagnetic cluster is saturated, a magnetic binding energy is possible as long as $\langle S \rangle_{cluster} > \langle S \rangle_{lattice}$. This situation is possible in the paramagnetic region of a magnetic material or below the magnetic ordering temperature in materials which do not order ferromagnetically. The bracketted term also explains the reduction in binding energy due to an applied field, since the latter tends to reduce the difference in average magnetization by increasing $\langle S \rangle_{lattice}$. With complete ferromagnetic order, metallic conduction is predicted at low temperatures for samples which are metallic at high temperatures. In our samples, where ferromagnetic alignment is not complete[24], the bound state represents a local region of full saturation and therefore, can exist to lowest temperatures. This is observed experimentally, in that the samples do not show metallic conductivity, but a magnetic field does tend to reduce the resistivity.

The model is also capable of explaining the qualitative features of the observed thermoelectric power. Of course, the simplest assumption to explain the temperature dependence of the thermopower is that $\sigma(E) \to 0$ below the mobility edge, E_c. This means that we set $E_x = E_c$ in Eq. 2.1.7, in which case S has as its leading term $(k/e)(E_c - E_F)$. Substitution of ΔE (Fig. 5) for $E_c - E_F$ gives a peak in the thermopower slightly above Θ as observed. However, the peak value of S predicted from ΔE is approximately twice as large as found experimentally for sample 2. The discrepancy is even larger for sample 3. Eq. 2.1.7 is not valid for sample 4, since the measured S is smaller than k/e. One possible explanation for this inconsistency is to assume, as did Cutler and Mott[15], that E_x the energy below which

$\sigma(E)\to 0$, is below E_c (as is indicated in Fig. 1). In this case ΔE would include both a term $E_x - E_F$ and an activation energy for hoppping, W. S, on the other hand, would be dominated at low temperatures by the first term in Eq. 2.1.7, which does not include W. The hopping energy would then be the difference between ΔE and S, at least for samples 2 and 3.

With the use of the bound magnetic polaron model, a natural explanation which does not involve an arbitrary cutoff in energy, is possible. If E_F is below E_c, then for temperatures such that $|E_c - E_F| >> kT$, transport of electrons occurs by hopping near E_F with conductivity given approximately by

$$\sigma \approx e^2 p R^2 N(E_F), \quad [34] \qquad 2.3.4$$

where R is the distance covered by each hop, and p is given by

$$p = (\nu_{ph} \exp(-2\alpha R)][\exp(-W/kT)] \qquad 2.3.5$$

Here ν_{ph} is the factor depending on the phonon spectrum, $\exp(-2\alpha R)$ is a factor depending on the overlap between localized states and W is the difference in energy between the occupied and unoccupied state. At relative high temperatures but still small enough so that only the electron distribution near E_F contributes to transport the first term in Eq. 2.3.5 remains constant and the conductivity is thermally activated with activation energy W. At lower temperatures variable range hopping occurs and both $\exp(-\alpha R)$ and W change. Mott has shown that this leads to his well known $T^{-1/4}$ law. It should be noted, however, that the physical process for both temperature ranges can be regarded as phonon assisted tunneling. The changes in the observed activation energy reflect the fact that at low temperatures only very few phonons are available to facilitate the hop. If we follow the

reasoning of Thompson et al[11] we can regard the electron motion as being defined by the average barrier height of the potential well, i.e. the distance from E_F to E_c. Thompson et al find that the high temperature value for W can be used to predict α, the decay of the bound electron wave function outside the potential well, and consequently, the low temperature variable range hopping behavior. We can, therefore, identify the measured activation energy, ΔE, with the distance $E_c - E_F$. This binding energy is dominated, at low temperatures by the magnetic term, with electrons hopping from site to site as described above.

Fritzsche[35] has pointed out that the thermopower has a simple physical meaning since it is related to the Peletier coefficient π as $S=\pi/T$. π is defined as the energy carried by the electrons per unit charge and the thermopower thus depends very sensitively on the total energy transport per carrier, either directly or by interactions with other normal modes of the system. This accounts for the phonon and magnon drag effects often encountered in metals. It also apparently accounts for the difference in activation energies observed by Emin et al[36] in their studies of α and S in chalcogenide glasses. These workers interpret the result that the activation energy ΔE_σ is larger than ΔE_S as being due to small dielectric polaron formation. The physical idea is that the excess charge carrier relaxes to a lower energy state by exchanging energy with the lattice (through small lattice distortions) forming the small polaron. In order to move, it has to overcome an energy barrier roughly equal to the polaron binding energy, W_H. If no net energy is transported in the hopping process, however, the hopping contribution to S is 0. Justification for the latter

assumption has been given by e.g. Austin and Mott.[37] They point out, however, that this result is only true if the total activation energy is equally divided between the two hopping sites. If the two sites are not equivalent a term cW_H/kT enters the thermopower. c is a constant much smaller than one[37] and reflects the inequavelence of the sites.

We view the thermopower results (Fig. 4) as being analogous to the above description. The trapped magnetic polaron binding energy in $Gd_{3-x}v_xS_4$ is a distribution of energies because of static fluctuating potentials caused by the disordered vacancies. We may expect, therefore, a finite contribution to S from the term cW_H/kT. We expect, furthermore, the anomalous peak in the thermopower to be quenched in the presence of a large magnetic field because the bound state requires both the coulombic and magnetic interaction to be stable. Experiments to verify this prediction are underway and preliminary results indicate a decrease in the thermopower peak with applied magnetic field.

3.0 MAGNETIC SUSCEPTIBILITY OF EXCHANGE COUPLED VAN VLECK IONS: $Sm_{1-x}La_xS$

3.1 INTRODUCTION

For the six 4f electrons of both Eu^{3+} and Sm^{2+}, Hund's rules indicate that L = 3 and S = 3; i.e. a ^7F term. Furthermore, the spin-orbit interaction favors an antiparallel coupling between $\vec{L}$ and $\vec{S}$, leaving the J = |L-S| = 0 state lowest; i.e. $^7F_0$. Since for such ions (Van Vleck ions) the ground state is <u>non-magnetic</u> (J=0), their magnetic properties are determined by the higher lying multiplet levels (J>0). The magnetic properties of these levels are manifested in two ways: at finite temperatures these levels are thermally populated; and, an external magnetic field

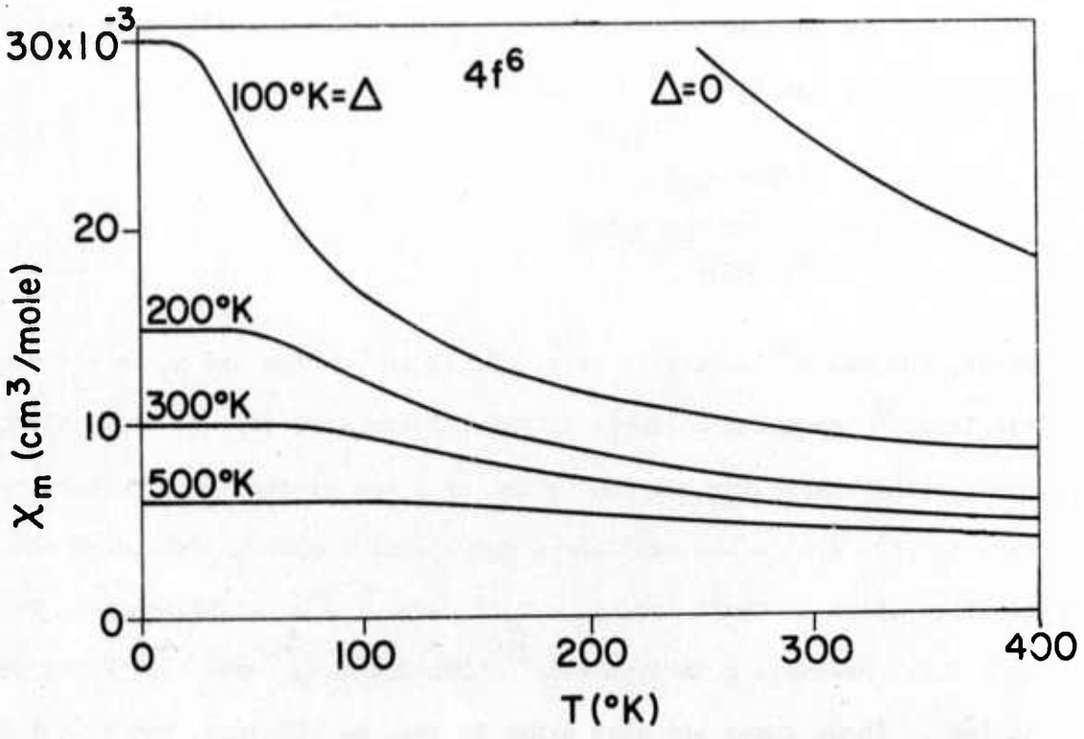

Figure 6 The temperature dependence of the magnetic susceptibility of a $4f^6$ Van Vleck ion calculated from Eq. 3.2.1 for various values of the spin-orbit coupling, Δ.

admixes the J=0 and J=1 levels, giving rise to a moment in the ground state. Both effects may be examined by measuring the magnetic susceptibility of these ions. In this paper we describe how such susceptibility measurements can be used to measure the exchange interactions between Van Vleck ions; in particular, the changes in the Sm^{2+}-Sm^{2+} interactions in SmS caused by conduction electrons.

3.2 SUSCEPTIBILITY OF A VAN VLECK ION

The magnetic susceptibility of such non-magnetic ions was first calculated by Van Vleck,[38] who found:

$$\chi = \frac{\sum_J (2J+1)\chi_J e^{-E_J/kT}}{\sum_J (2J+1) e^{-E_J/kT}} \qquad 3.2.1$$

where, for the J^{th} multiplet level, E_J is the energy and χ_J is the susceptibility.[38] Assuming a simple spin-orbit coupling (Δ), we have calculated the susceptibility for various values of Δ and plotted them versus temperature in Fig. 6. In the case of no spin-orbit coupling (Δ=0), the susceptibility obeys a Curie law, $\chi_M = C_M/T$, as for a usual paramagnet, with $C_M = 7.5$. However, Δ is typically[39] $\sim$500°K for Eu^{3+} and $\sim$300°K for Sm^{2+} in SmS[3]. These cases are also shown in Fig. 6. Clearly, the effect of the spin-orbit coupling is to dramatically reduce the susceptibility, by tending to align $\vec{L}$ antiparallel to $\vec{S}$, thus reducing the effective moment.

The temperature dependence of χ_M contains contributions due to both effects mentioned earlier: at high temperatures, the higher lying multiplet levels are thermally populated but χ_M decreases with increasing

T as the Curie law susceptibility of these moments decreases. At lowest temperatures, the thermal population of the higher multiplets is negligible and χ_M is dominated by the moment admixed from J=1 by the applied magnetic field. This contribution to χ_M is the Van Vleck temperature independent susceptibility:[38,41]

$$\chi_{vv} = \chi_M(0) = 8N\beta^2/\Delta \qquad 3.2.2$$

where Δ is more generally defined as the energy difference between the J=0 and J=1 states. Thus the low temperature value of χ_M can be used as a direct measure of Δ (Eq. 3.2.2 and Fig. 6).

3.3 EFFECTS DUE TO EXCHANGE

In the absence of an applied magnetic field, the exchange interactions between Sm^{2+} ions do not affect the J=0 ground state, since it has no moment. There will, however, be effects on the excited states which can be measured by the susceptibility. An early discussion of these effects is given by Bozorth and Van Vleck[39] for exchange interactions between Eu^{3+} ions. More recently, susceptibility measurements by Bucher, Narayanamurti and Jayaraman[42] revealed large differences in $\chi_M(0)$ between SmTe, SmSe, and SmS. It was suggested by Mehran, et al[43] and by Birgeneau, et al[40] that these differences were due to different Sm^{2+}-Sm^{2+} exchange interactions. Using molecular field theory, Birgeneau, Bucher, Rupp and Walsh[40] showed that the exchange interactions between Sm^{2+} ions alter the splitting, Δ, between the J=0 and J=1 states, so that Eq. 3.2.2 becomes:

$$\chi_M(0) = \frac{8N\beta^2}{\Delta_o - 8\sum z_i J_i} \qquad 3.3.1$$

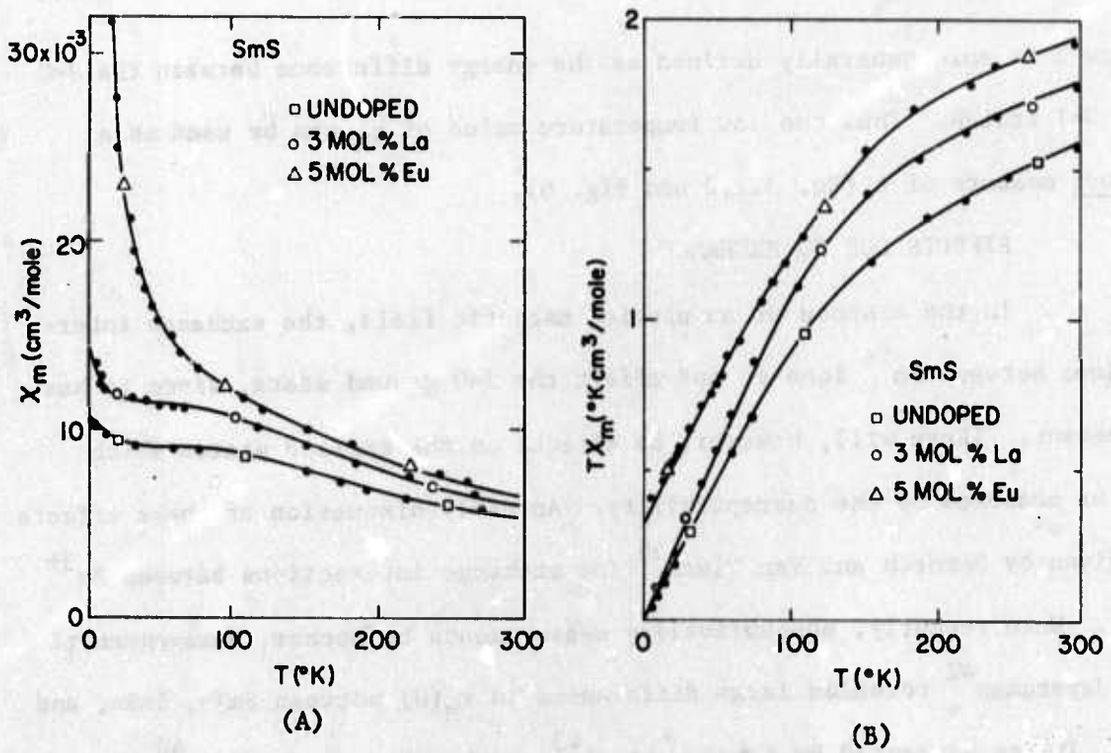

Figure 7 (a) The susceptibility per mole Sm measured for three samples of SmS showing the paramagnetic impurity contribution at lowest temperatures. (b) A plot of $T\chi_M$ for the same three samples showing the straight line behavior below ∿75°K predicted by Eq. 3.4.1.

where the change in Δ from Δ_o is caused by the exchange interaction J_i between z_i neighbors. For a ferromagnetic exchange, this reduction in Δ gives rise to an increase in $\chi_M(0)$. Birgeneau, et al[40] have used Eq. 3.3.1 with Δ_o=415°K to obtain the values for the Sm^{2+}-Sm^{2+} exchange interactions in SmTe, SmSe and SmS. In this section we report measurements of the increase in the Sm^{2+}-Sm^{2+} exchange interaction in SmS caused by conduction electrons.

The exchange interactions between Sm^{2+} ions and impurity spins (e.g. Eu^{2+}, Mn^{2+} and Gd^{3+}) have also been observed by Mehran, et al[43], by Birgeneau, et al[40], and by Walsh, et al[44] in SmTe, SmSe and SmS by measuring the large EPR g-shifts.

3.4 EFFECTS OF PARAMAGNETIC IMPURITIES

Since the variations in the exchange interactions that we expect to measure are small compared to Δ_o, the changes in $\chi_M(0)$ will be correspondingly small (Eq. 3.3.1) and particularly accurate measurements will be necessary. Also since the spin-orbit coupling greatly reduces χ_M (Fig. 6), a relatively small amount of paramagnetic impurities can have an important effect on our measurement of the exchange interaction. Samples of SmS generally have as much as 0.1% impurities, largely originating from the commercial Sm metal used in the synthesis. As an example, the measured χ_M data for two samples of average purity are shown in Fig. 7a: one undoped and one with nominally 3% La (La^{3+} is diamagnetic). Note the rise in χ_M at lowest temperatures which is presumably caused by paramagnetic impurities. Since the difference in $\chi_M(0)$ between these two samples is nearly the largest we have found, we must be able to accurately measure smaller changes

in $\chi_M(0)$ and hence we must subtract off the impurity contribution from the data. Also included in Fig. 7a is a sample of SmS intentionally doped with nominally 5% Eu. In this extreme case, the Eu^{2+} paramagnetic susceptibility completely obscures the temperature independent part of χ_M.

In order to eliminate the impurity contributions we assume that the impurities are purely paramagnetic (i.e. $\chi \sim C/T$). We then examine the product of T times the total measured susceptibility:

$$T\chi_M = 8N\beta^2 T/\Delta + C \qquad 3.4.1$$

Thus, a plot of $T\chi_M$ versus T should give a straight line at low temperatures, with a slope related to Δ and a T=0°K intercept which measures the impurity contribution. Such a plot for each of the three samples of Fig. 7a is shown in Fig. 7b. Note that even for the 5% Eu sample we get a straight line. For that sample, the T=0 intercept converts to a Eu^{2+} concentration of 4.5% and the value of Δ obtained from the slope is 346°K, compared to ~335°K for SmS. On the other hand, the value of Δ for the 3% La sample is 273°K and reflects the large increase in the exchange interaction caused by the conduction electrons donated by the La. The T=0°K intercepts for the two samples without intentional Eu doping indicate, for example, that if all the impurities were Eu^{2+}, there would be a 0.15% concentration.

3.5 La DOPED SmS

Since La in SmS is expected to be in the trivalent state, each La should add one conduction electron to the system, which will give rise to an indirect interaction between Sm^{2+} ions. Since La^{3+} itself is diamagnetic with about the same diamagnetic susceptibility as Sm^{2+}, the susceptibility behavior of La doped SmS should be similar to undoped SmS: any

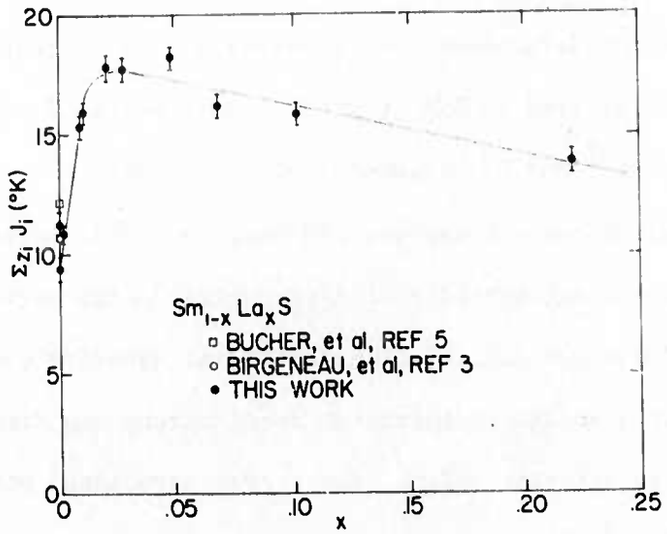

Figure 8 The Sm^{2+}-Sm^{2+} exchange interaction in La doped SmS showing the increase in the exchange due to the conduction electrons. The error bars represent a $\pm 1/2\%$ error in the measurement of χ_M.

changes in χ_M (per mole Sm) will then be attributed to changes in the Sm^{2+}-Sm^{2+} exchange interaction caused by the conduction electrons. Using the techniques described above, we have obtained the sum of the exchange interactions between Sm^{2+} ions, $\sum z_i J_i$, for a series of samples with differing La concentrations. The results are plotted in Fig. 8, with the error bars on the data points representing a ± 1/2% error in χ_M.

Also plotted in Fig. 8 are the data points for undoped SmS obtained by Bucher, et al[42] and by Birgeneau, et al[40]. Note the variation between these two samples and our two undoped samples. This variation probably represents to a large extent real differences in the exchange interactions caused by differences in stoichiometry and/or impurity content, since we shall see that a small concentration of electrons can dramatically increase the exchange interaction. Thus, the errors associated with these effects although difficult to estimate are probably larger than the error bars in Fig. 8.

The major feature of the data in Fig. 8 is that the exchange interactions suddenly increase with increasing La concentration, so that near 3% La they are <u>almost</u> <u>twice</u> the value of undoped SmS. Further increases in the La concentration cause the exchange to decrease.

4.0 RARE EARTH INTERCALATION AND MAGNETIC PROPERTIES OF LAYER TYPE COMPOUNDS

4.1 INTRODUCTION

The transition metal dichalcogenides of group IV, V and VI form layer type compounds where a single layer consists of metal ions strongly bonded between two sheets of chalcogens.[45] Adjacent layers are weakly bonded to each other, presumably by van der Waals forces, making it possible

to place other ions or molecules in the gap between the layers without disturbing the ionic arrangement within a given layer. This process is called intercalation. Distinct changes in the physical properties of the host layer material usually occur as a result of intercalation, presumably due to electron exchange between the intercalated species and the host.

There has been some previous work on the intercalation of magnetic ions into the gap of these structures, mainly putting in 3d metals by high temperature reactions[46-49]. In such cases structures with many three dimensional characteristics are formed. Rudorff[50,51], however, showed that europium, since it is soluble in liquid ammonia, can be intercalated at low temperatures in a manner similar to the alkali metals. Further, from susceptibility measurements he showed the intercalated europium to be in the divalent state.

In this section we present further data on the intercalation and properties of europium in MoS_2, we show that ytterbium and strontium can also be intercalated, and we compare the magnetic properties of the three intercalated systems.

4.2 EXPERIMENTAL

The layer dichalcogenides were prepared as powders by the direct reaction of the elements in sealed silica tubes. The resulting powders were used as source material for crystal growth runs by the chemical vapor transport technique. Iodine was used as the carrier in most runs. The 3R polytype was obtained in all cases. The intercalations were carried out by reacting either the powders or crystal with liquid ammonia solutions of the metals i.e., Eu, Yb, or Sr. The solutions had the deep blue color

characteristic of free solvated electrons in ammonia and the intercalation process was considered complete when the solution became colorless. The rate of intercalation, as determined by the time required for the solution to become colorless, depended on the usual parameters such as temperature, concentration and particle size of the dichalcogenides. However, the primary rate determining parameter for this experiment was the particle size of the material being intercalated. For example, at -50°C small crystals were not completely intercalated after 16 weeks in solution whereas fine powders (~3000Å) showed complete intercalation after several days. Temperature had a lesser but still significant effect on the reaction rate. We were restricted in the temperature range in which the intercalation could be carried out because at higher temperatures i.e., room temperature, there was a tendency for the formation of europium amide ($Eu(NH_2)_2$[52], - a ferromagnet which we could not tolerate as an impurity. Therefore, all reactions were carried out at low temperatures (-70 to -50°C) where amide formation did not occur. After the intercalation was complete the samples were washed in freshly distilled NH_3, dried in high vacuum, and then transferred to a dry box where they were removed from the reaction tube and mounted for the various examinations.

All samples were analyzed chemically for both europium and ammonia. The europium was determined by EDTA to an accuracy of $\pm$ 1% while the ammonia was done colorimetrically using Nesslers reagent. The magnetic measurements were made with a force magnetometer.

4.3 RESULTS AND DISCUSSION

The results of the intercalation from liquid ammonia solutions

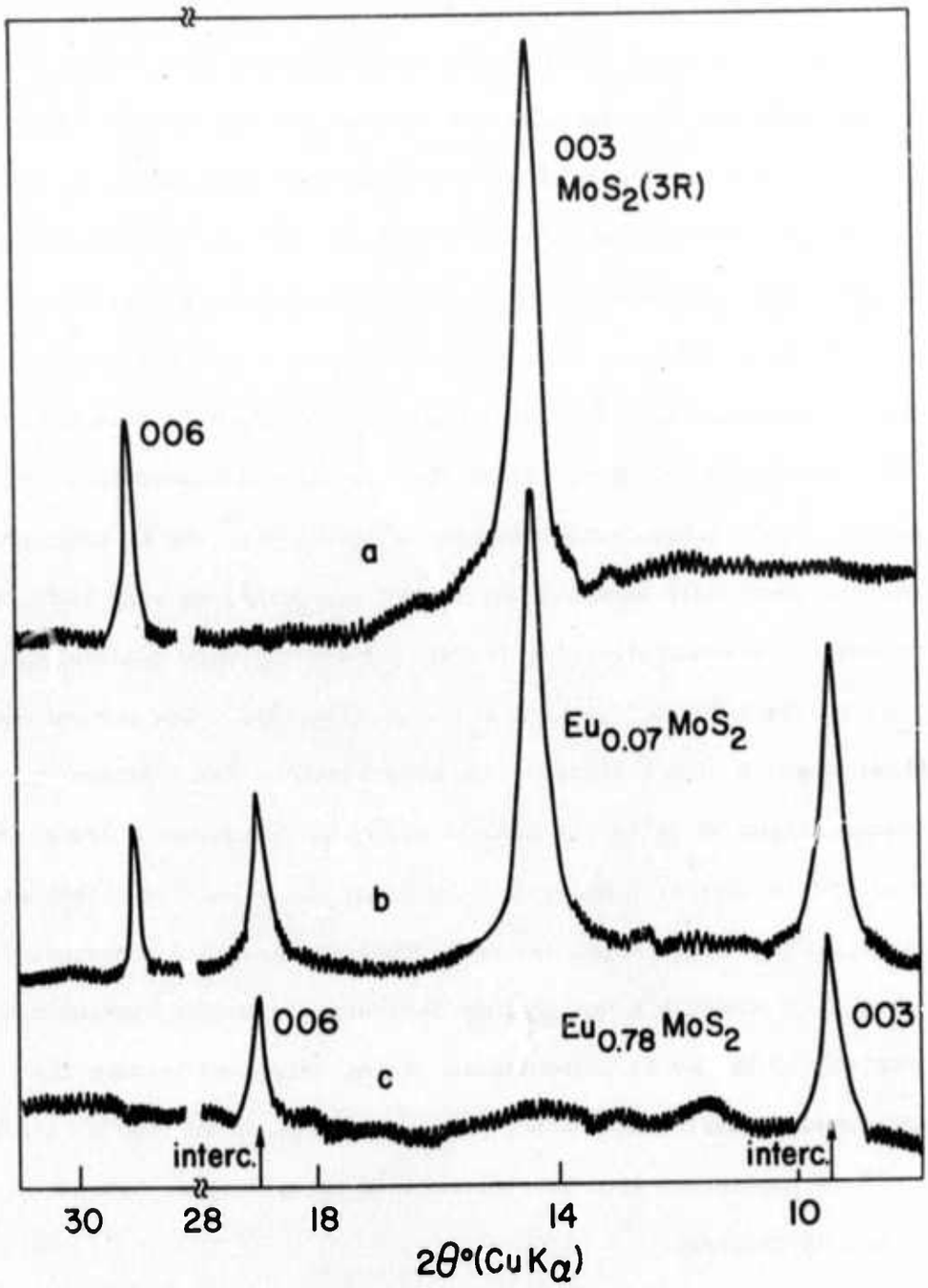

Figure 9 X-ray diffraction patterns of (a) MoS_2(3R) and (b and c) Eu intercalated MoS_2. At low Eu concentrations both intercalated and pure phases are present (b and c) and the 003 peak intensities vary with the Eu concentration.

are summarized in Table II. There are several significant points which warrant further emphasis. First; ammonia is always found intercalated with europium. The ratio of Eu to NH_3 varied between ~0.8 to 2.5 but the scatter in the analyses does not allow us to draw any conclusions as to the composition of the complex which is intercalated. However, in no cases could ammonia be intercalated without europium. Second; the lattice parameters in all cases are idential and independent of the concentration of the intercalated material. This means that when two layers separate to accept the intercalated species, the amount of separation is determined only by the size of this species. Since the low concentrations show the same spacing as the highly concentrated ones it is likely that the Eu concentration necessary to completely separate two layers (to 3.15Å) is very low. For the low concentrations mixtures of intercalated and the pure intercalated phase are seen in the X-ray diffraction tracings (Fig. 9b). The percent intercalated phase shows a linear increase (as determined by X-ray intensity data) as the concentration of Eu in the ammonia solution is increased and at $MoS_2(Eu)_{.58}$ only the intercalated phase is seen (Fig. 9c). We assume that at this concentration every layer has been separated by small concentrations of ammoniated europium's and further increases in the Eu content can be accounted for by the Eu concentration being increased between the previously separated layers. The lattice parameter increase in the c dimension of 9.45Å is consistent with an intercalated species being between every layer of the 3R polytype.

Attempts were made to intercalate Eu and Sr into MoS_2 by solid state reactions at 400-800°C by reacting the metals with MoS_2 in evacuated

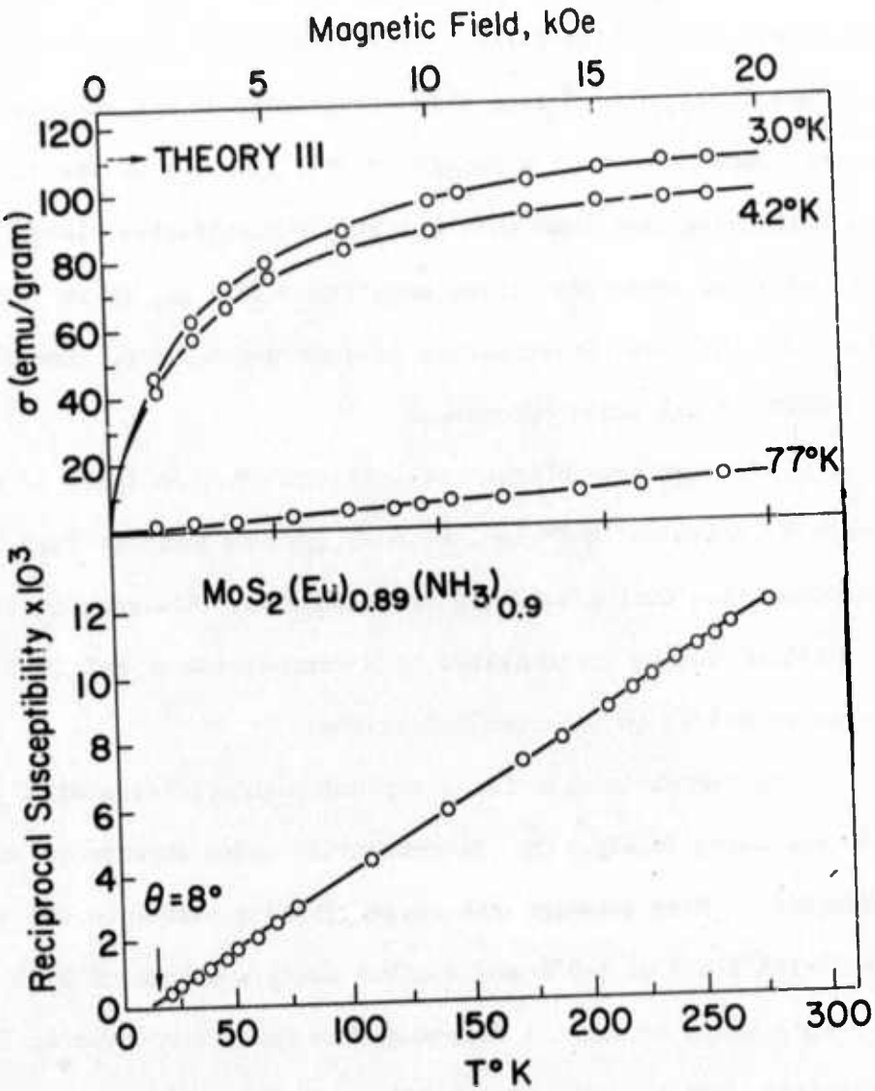

Figure 10 Magnetic data on $MoS_2(Eu_{.89}(NH_3)_{.9}$.

silica tubers. Negligible amounts of Eu and about 25% Sr were intercalated. The lattice constants of these compositions were a_o=3.20Å and c=3x7.19Å. However, in all cases the corresponding metal sulfides were formed.

It is also evident from Table II that the maximum concentration of intercalated europium in MoS_2 corresponds to a composition of approximately $MoS_2(Eu)_{.95}$; to obtain this composition it was necessary to have a starting composition with a MoS_2/Eu = .75. In view of the fact that solutions containing less than this starting concentration always become decolorized while those containing more remained blue, it is difficult to explain why the final intercalated product was found to contain approximately only 70-80% of the added europium.

Although some of the compositions given in Table II show the presence of trivalent europium, we have data to indicate this is a result of decomposition during handling and measuring. However, it is evident that europium can be intercalated to a composition of $MoS_2(Eu) \sim 1$ and that it is intercalated in the divalent states.

The magnetic data for a typical highly intercalated (with Eu) sample are shown in Fig. 10. Ferromagnetic order appears to occur at low temperatures. From paramagnetic susceptibility values in the temperature range 77-298°K a Θ of 8-9°K and a molar Curie constant of 7.88 for Eu^{++} with a spin value of 7/2. A ferromagnetic Curie temperature, T_c, of 4-5°K was obtained from initial permeability measurements. Several low temperature magnetization curves for this functional dependence of the moment versus field shows some characteristics of ferromagnetic order.

TABLE II

Starting Composition Moles MoS_2: T	Final Composition (from Analyses)	Lattice Parameter* C_o, Å	Paramagnetic Curie temperature θ, °K	Molar Curie Constant C_M
1:0	MoS_2	3 x 6.13		
1:0.2 Eu	$MoS_2(Eu)_{0.07}(NH_3)_{0.15}$	3 x 9.28	-10 ± 5†	3.1
1:0.5 Eu	$MoS_2(Eu)_{0.38}(NH_3)_{0.29}$	"	0 ± 1	8.1
1:0.75 Eu	$MoS_2(Eu)_{.58}(NH_3)_{1.3}$	"	4 ± 4†	7.1
1:1.0 Eu	$MoS_2(Eu)_{.74}(NH_3)_{2.1}$	"	-†	6.0
1:1.0 Eu	$MoS_2(Eu)_{.78}(NH_3)_{1.7}$	"	9 ± 2	6.9
1:1.2 Eu	$MoS_2(Eu)_{.89}(NH_3)_{.9}$	"	8.8 ± 1	7.9
1:0.2 Yb	$MoS_2(Yb)_{0.1}(NH_3)_{.16}$	3 x 9.21	-	-
1:0.2 Sr	$MoS_2(Sr)_{.11}(NH_3)_{.4}$	3 x 9.28	-	-

*The a_o lattice parameter for all intercalated materials is 3.20 Å as compared with 3.16 Å for pure MoS_2. There were no superlattice lines observed which could be used to indicate the position of the intercalated ions.

†The presence of trivalent europium in the samples decreases the accuracy of the extrapolation from high temperature of the $1/\chi$ versus T curve because of the deviations from a straight line.

However, the fact that complete saturation, as evidence by the slope of the M-H curve, does not occur up to ∿15 kOe indicates either a complex spin structure or the presence of a paramagnetic phase. If the latter were the case the data indicates it should be present in the 20-25% range - a fact which is inconsistent with the X-ray and the susceptibility data. The presence of $Eu(NH_2)_2$[52] or $Eu(NH_3)_6$[53] as ferromagnetic impurities is also ruled out by the X-ray measurements. A spin arrangement in which the europiums are coupled ferromagnetically within a sheet and adjacent sheets being coupled antiferromagnetically could account for the shape of the magnetization curve. In such an arrangement the dipolar exchange forces coupling adjacent layers are assumed to be weaker than the intra layer exchange so that only moderate fields i.e. 15-20,000 Oe are required to flip the spins to a parallel arrangement, as is seen in the magnetization curve at ∿15,000 Oe. The fact that the saturation moment is within a few per cent of theoretical for this composition (104 vs 111 emu's) shows that all Eu spins are ferromagnetically aligned.

Those samples intercalated with europium concentrations less than about $MoS_2(Eu)_{.4}$ have either zero or slightly negative paramagnetic Curie temperatures. The M versus H curve for the $MoS_2(Eu)_{.38}$ sample shows some characteristics of ferromagnetism at 2°-4.2°K but since this sample was a mixture of intercalated and pure MoS_2 we assume it contained small regions with sufficiently high Eu concentration for magnetic order to occur. It appears, that for homogenous samples, a europium concentration in the 0.4 - 0.5 Eu to one MoS_2 is necessary for ferromagnetism.

Strontium and ytterbium intercalated samples with increased

lattice parameters identical to the europium ones were also prepared. No evidence of ferromagnetism was observed in these, which is good evidence showing the origin of the magnetism in the Eu sample is in the Eu layer and not the molybdenum. In fact both the Sr and Yb samples became superconducting at 5.2 and 3°K respectively. This is presumed to be a result of electrons from the intercalated species being transferred to the d band of the MoS_2.

REFERENCES

1. T. Kasuya and A. Yanase, Rev. Mod. Phys. 40, 684 (1968).
2. T. Kasuya, in "Proc. 10th Int. Conf. on the Physics of Semiconductors, Cambridge, Mass., 1970," S. P. Keller, J. C. Hensel and F. Stern, eds., CONF-700801 (U.S. AEC Div. of Tech. Info., Springfield, Va., 1970), p. 243.
3. J. B. Torrance, M. W. Shafer, and T. R. McGuire, Phys. Rev. Letters 29, 1168 (1972).
4. See, e.g. N. F. Mott and E. A. Davis, "Electronic Processes in Non-Crystalline Materials" (Clarendon Press, Oxford, 1971).
5. P. W. Anderson, Phys. Rev. 109, 1492 (1958).
6. J. A. van Vechten, Solid State Commun. 11, 7 (1972).
7. D. T. Pierce and W. E. Spicer, Phys. Rev. B5, 3017 (1972); W. E. Spicer and T. M. Donovan, J. Non-Cryst. Solids 2, 66 (1970).
8. G. Busch, M. Campagna and H. C. Siegmann, to be published.
9. D. Redfield, J. Non-Cryst. Solids 89, 602 (1972).
10. D. Redfield and R. S. Crandall, "Proc. 10th Int. Conf. on the Physics of Semiconductors, Cambridge, Mass., 1970," S. P. Keller, J. C. Hensel and F. Stern, eds., CONF-700801 (U.S. AEC Div. of Tech. Info., Springfield, Va., 1970), p. 574.
11. W. A. Thompson, T. Penney, S. Kirkpatrick, and F. Holtzberg, Phys. Rev. Letters 29, 779 (1972).
12. Ref. 4, pg. 42.
13. M. Cutler, J. F. Leavy, and R. L. Fitzpatrick, Phys. Rev. 133, A1143 (1964).

14. M. Cutler and J. F. Leavy, Phys. Rev. 133, A1153 (1964).

15. M. Cutler and N. F. Mott, Phys. Rev. 181, 1336 (1969).

16. Landbolt-Börnstein Tables, K. H. Hellwege and A. M. Hellwege eds., 4a, pp. 41-109, Springer-New York (1970).

17. K. Meisel, Z. Anorg. Chem. 240, 300 (1939).

18. W. H. Zachariasen, Acta Cryst. 2, 57 (1949).

19. P. I. Kripyakevich, Soviet Physics-Cryst. 7, 556 (1963).

20. F. Holtzberg and S. Methfessel, Journ. of Applied Physics 37, 1433 (1946).

21. F. Holtzberg, Y. Okaya and N. Stemple, Amer. Crystallogr. Ass. Meeting, Gaithersburg, Tenn. p. 46 (1965).

22. W. L. Cox, H. Steinfink and W. F. Bradley, Inorg. Chem. 5, 318 (1966).

23. F. L. Carter, J. Solid State Chem. 5, 300 (1972).

24. S. von Molnar, F. Holtzberg, T. R. McGuire and T. J. A. Popma in "AIP Conference Proc. 5," C. D. Graham and J. H. Ryne, eds. p. 869 (1972).

25. E. H. Putley, "The Hall Effect and Related Phenomena," Butterworth, London (1960).

26. Olof Lindberg, Proc. I.R.E. 40, 1414 (1952).

27. Y. Shapira and T. B. Reed, Phys. Rev. B5, 4877 (1972).

28. W. Thompson, private communication.

29. S. von Molnar, to be published.

30. T. Penney, M. W. Shafer, and J. B. Torrance, Phys. Rev. B, 5, 3669 (1972).

31. It is clear that little meaning can be attached to the magnitudes of the derived energies away from the peak near 200°K. Both the term f(1-f) and the magnetic localization energy are competing to produce an effective ΔE. But near the peak, $\Delta E >> kT$ and is a good measure of the activation energy.

32. J. Torrance, private communication.

33. Without the Coulomb interaction, the magnetic polaron in a ferromagnetic is stable only very close to the magnetic ordering temperature [c.f. T. Kasuya, A. Yanase, and T. Takeda, Solid State Commun. 8, 1543 (1970)].

34. Ref. 4, Eq. 2.36.

35. H. Fritzsche, Solid State Commun. 9, 1813 (1971).

36. D. Emin, C. H. Seager, and R. K. Quinn, Phys. Rev. Letters 28, 813 (1972).

37. I. G. Austin and N. F. Mott, Advances in Physics 18, 41 (1969).

38. J. H. Van Vleck, Theory of Electric and Magnetic Susceptibilities (Oxford Univ. Press., London 1932) Ch. IX.

39. R. M. Bozorth and J. H. Van Vleck, Phys. Rev. 118, 1493 (1960).

40. R. J. Birgeneau, E. Bucher, L. W. Rupp, Jr., and W. M. Walsh, Jr., Phys. Rev. B 5, 3412 (1972).

41. For Δ in units of °K and χ_M in units of cm^3/mole, Eq. (2) can be written $\chi_M(0) = 3.0093/\Delta$.

42. E. Bucher, V. Narayanamurti, and A. Jayaraman, J. Appl. Phys. 42, 1741 (1971).

43. F. Mehran, K. W. H. Stevens, R. S. Title, and F. Holtzberg, Phys. Rev. Letters 27, 1368 (1971).

44. W. M. Walsh, Jr., L. W. Rupp, Jr., R. J. Birgeneau and L. D. Longinotti, A.I.P. Conf. Proc. 10 (1973).

45. See recent review by J. A. Wilson and A. O. Yoffe, Advan. Phys. 18, 193 (1969).

46. F. Hulligar and E. Pobitschka, J. Solid State Chem. 1, 117-119 (1970).

47. J. M. Voorhoeve-van den Berg and R. C. Sherwood, J. Phys. Chem. Solids 1, 134-137 (1970).

48. J. M. Voorhoeve-van der Berg and R. C. Sherwood, J. Phys. Chem. Solids 32, 167-173 (1971).

49. K. G. Verhoeven, thesis Groningen 1971.

50. W. Rüdorff, Chimia 19, 489-499 (1965).

51. W. Rüdorff and W. Ostertag, Proc. IV Rare Earth Res. Conf. Phoenix, Arizona (1965).

52. F. Hulliger, Solid State Comm. 8, 1477-1478 (1970).

53. H. Oestereicher, N. Mammano and M. J. Senko, J. Solid State Chem. 1, 10-18 (1969).